



preference for the triaxial C–F conformer with di- and tri-alkylated derivatives. This is predicted by the computational outcomes presented in Fig. 1 for cyclohexanes **3** and **4**. Progressive methylation at alternate positions around the ring is predicted to increase the triaxial C–F preference and increase the bias towards the more polar arrangements. The calculated<sup>7</sup> molecular dipole moments ( $\mu$ ) for the conformers of **4** indicate that it is the triaxial arrangement of the fluorines which contributes most significantly to molecular polarity ( $\mu = 4.65$  D), the ring inverted conformer with equatorial fluorines is much less polar ( $\mu = 1.01$  D). With this background it became an objective to prepare a range of all-*syn* 2,4,6-trialkylated-1,3,5-trifluorocyclohexanes **16**, to assess their structures and properties, particularly as they are predicted to be strongly trifluoro-triaxial with the more polar conformations dominating. A general route was devised to this class of compounds which also allowed mono- and di-alkylated cyclohexane rings of this class to be prepared as shown in Scheme 1.

The syntheses sequences start with Sonogashira protocols<sup>8</sup> coupling the appropriate commercially available fluoriodobenzene **5**, **9** or **13** with terminal acetylenes. The resultant aryl-acetylenes **6**, **10a–c** or **14a–f** were then hydrogenated under standard conditions over Pd/C to generate alkyl-fluoroaryls **7**, **11a–c** or **15a–f** respectively with saturated side chains. These products were then subject to aryl ring hydrogenations under the conditions recently reported by Glorius<sup>8</sup> for the preparation of fluorocyclohexanes from aromatic precursors, using the [CAAC]-COD Rh catalyst **17**.<sup>9</sup> Although these aryl hydrogenation reactions proved to be slow ( $H_2$ , 50–70 bar, 1–10 d) conversions overall are moderate to good and it offered a direct approach to this class of compounds generating products **8**, **12a–b** and **16a–f** as illustrated in Fig. 2. Some of the products were amenable to X-ray structure analysis, such as the monosubstituted derivative **8**, the disubstituted derivative **12c** and trisubstituted trifluoro-cyclohexanes **16d**, **16e** and **16f**. The offset in the stacking arrangement of the fluorocyclohexyl rings, as observed for the

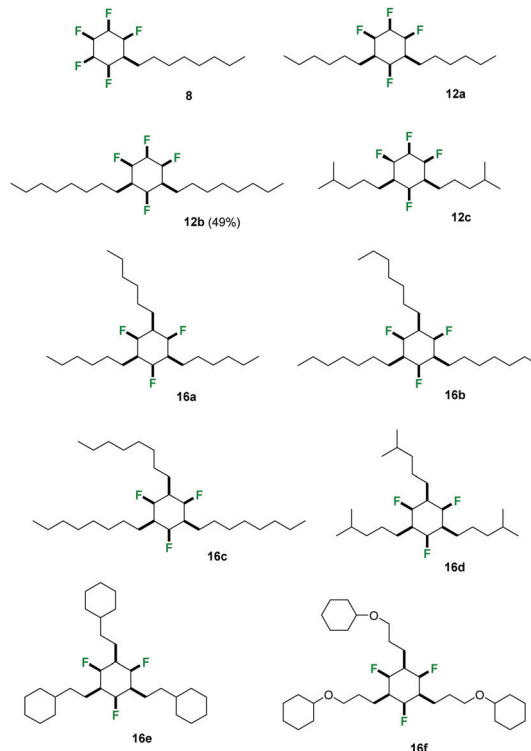
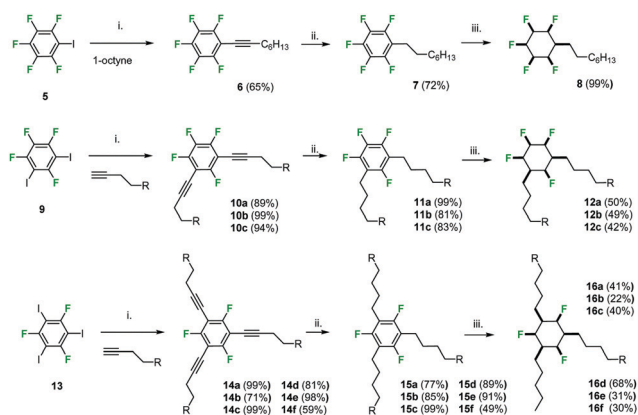


Fig. 2 Structures of the product mono-**8**, di-**12a–b** and tri-**16a–f** fluoroalkylated cyclohexanes prepared in this study.

monosubstituted derivatives<sup>2,6</sup> was not observed for the di- and tri-substituted systems.

On the other hand, in the cases of the di- and tri-substituted derivatives **12c**, **16d** and **16e**, the cyclohexane rings stack directly, one on top of another as illustrated in Fig. 3 for **16e** (see also Fig. S16–S18, ESI<sup>†</sup>). It is also interesting to note that the alkyl substituents in the di- and tri-substituted systems lie in the plane of the stacked rings very different to the monosubstituted all-*syn* pentafluorocyclohexyl systems such as **8** and as previously disclosed in other cases where there is an angular herringbone arrangement of the side chains to the rings in the solid-state.<sup>6a</sup> The more ordered stacking arrangement of the trialkyls **16** as a class was explored computationally in the dimeric and trimeric molecular assemblies for compound **4** as a model.

The surface electrostatic potential map for the triaxial arrangement of the fluorines in **4** as illustrated in Fig. 1,



**Scheme 1** Reaction conditions: (i) **5**, **9**, **13** (2.5 mmol); terminal alkyne (3–9 mmol), bis( $PPh_3$ )PdCl<sub>2</sub> (0.375 mmol), Cu(I)I (0.357 mmol), DIPA (25 mL), 80 °C, 24 h; (ii) **6**, **10**, **14** (0.3–2 mmol), 10% Pd/C (10% wt eq), hexane or MeOH (10–100 mL),  $H_2$  (3–15 bar), 20 °C, 16–72 h.; (iii) **7**, **11**, **15** (0.17–0.78 mmol), Rh(CAAC)-COD **17** (1.6 mol%), silica (0.2–1.6 g)/4 Å mol sieves (0.2–3.2 g), hexane (2–40 mL),  $H_2$  (50–70 bar), 25–50 °C, 1–10 d.

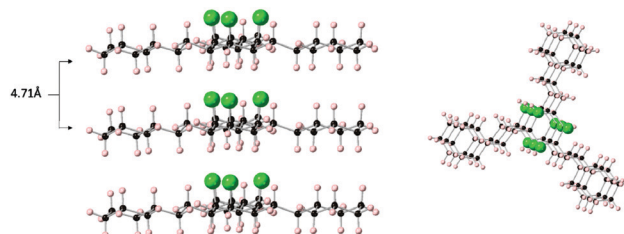


Fig. 3 Structure of **16e** showing perpendicular ring stacks in three isolated molecules.



highlights the Janus face character of this cyclohexane, with a highly negative (red) electrostatic potential associated with the triaxial fluorine face and a highly positive (blue) electrostatic potential associated with the triaxial hydrogens. On the other hand, the polarization diminishes considerably upon ring inversion, and the Janus face characteristic is lost for the triaxial alkyl groups in compound **4**. It is notable that the stacking of the cyclohexane rings in the tri-substituted derivatives further increases the attractive intermolecular interaction between positive and negative ring faces, as evidenced by the surface electrostatic potential maps for the dimer and trimer as illustrated in Fig. 4a, and by the interactions obtained through QTAIM and NCI calculations between axial fluorines and axial hydrogens (Fig. 4b and c, respectively).<sup>10</sup> The strong attractive F–H interactions significantly stabilize these arrangements, with calculated complexation energies for the dimer and trimer of  $-8.04$  kcal mol<sup>-1</sup> and  $-17.40$  kcal mol<sup>-1</sup> respectively, the latter value essentially being the sum of two such intermolecular interactions. Therefore, it can be anticipated that it is the array of F···H contacts which are responsible for stabilizing the intermolecular cyclohexane interactions, leading to stabilization of the crystalline supramolecular assembly of the trialkyl-substituted cyclohexanes.

Only in the trisubstituted structures **16** are the ring stacks completely insulated from each other by the alkyl substituents. In the mono- and di-substituted systems *e.g.* **8** and **12c** there is lateral contact between fluorocyclohexane ring stacks (see ESI†)

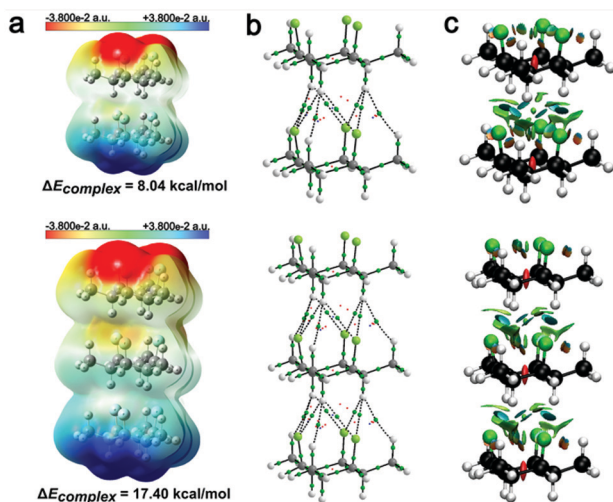


Fig. 4 (a) Surface electrostatic potential maps for dimeric and trimeric arrangements of the polar conformer of **4** obtained at the PBE0/def2-TZVP theory level. Both dimer and trimer are characterized by the electrostatic attraction between the hydrogen and fluorine faces. (b) QTAIM molecular graphics obtained from the PBE0/def2-TZVP electron density, with bond critical points (BCPs) represented by green spheres and ring critical points (RCPs) and cage critical points (CCPs) represented by small red and blue spheres, respectively. (c) NCI iso-surfaces obtained from PBE0/def2-TZVP electron density using reduced density gradient (RDG) = 0.5 and blue-green-red colour scale ranging from  $-0.015 < \text{sign}(\lambda_2)\rho(r) < 0.015$  a.u. Complexation energies were calculated at B3LYP-D3/def2-TZVP optimised geometries using the HFLD method and with the aug-cc-pVTZ basis set.<sup>10</sup>

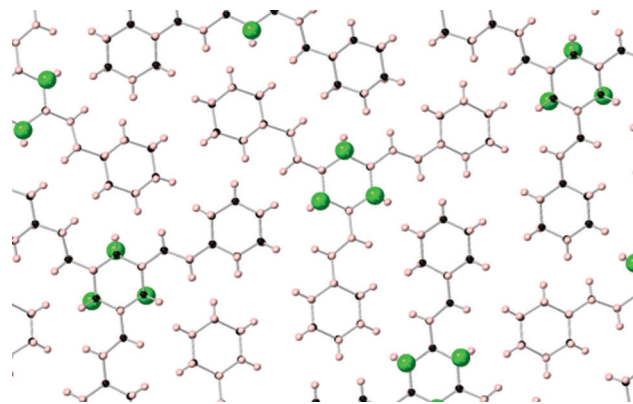


Fig. 5 The solid-state packing arrangements in the structure of **16e** showing that the all-*syn* fluorocyclohexane stacks are isolated and insulated laterally from each other by the hydrocarbon side chains. This is not the case for the mono- and di-substituted alkyl systems *e.g.* **8** and **12c** (see ESI†).

whereas there is a complete insulation of ring stacks in the solid-state structure of the trisubstituted compounds as illustrated for **16e** in Fig. 5. This suggests a characteristic of the trisubstituted systems in the solid-state.

Differential scanning calorimetry (DSC) and polarising optical microscopy (POM) analyses were carried out to assess if these materials were predisposed to polymorphism and/or liquid crystalline phases.<sup>11</sup> The analyses for compounds **16a–f** is presented in the ESI† and illustrated here for compound **16d** in Fig. 6. DSC analysis indicated that for some of the compounds only a single phase transition (melting point) was apparent, however for others, such as **16d**, there is clear polymorphic behaviour with a distinct transition at 97 °C prior to melting at 141 °C. The POM image of this polymorphic phase for **16d** has a clearly contrasted and highly orientated fibrous aspect typical of an ordered supramolecular structure, and this is found in several of the other systems too (see ESI† for **16a** & **16e**) although characteristics vary with different alkyl functionality.

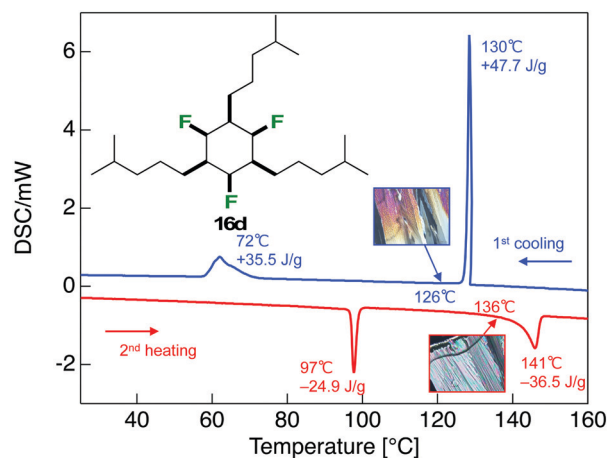


Fig. 6 DSC trace of **16d** illustrating polymorphic phases (mp = 141 °C) during the 1st cooling and 2nd heating cycle.



In conclusion we have presented a synthesis approach to selectively alkylated all-*syn* alkylated cyclohexanes that also contain triaxial C–F bonds, and we profile the alternating 2,4,6-trialkyl motifs in particular. The parallel orientation of the C–F bonds imparts a high polarity to these ring systems, and in selected cases the alkyl chains completely insulate the Janus ring stacks from each other, an arrangement which is not observed for the mono- and di-alkylated systems. The predisposition of the polar Janus rings to assemble in stacks due to electrostatic attraction between the alternating faces of the rings holds promise for ordering supramolecular assemblies with polar properties and offers an approach to designing next generation soft materials such as polar liquid crystals.

We thank the EPSRC for a studentship (TJP) through the CRITICAT Doctoral Training Centre. FAPESP is also gratefully acknowledged for a studentship (BAP, #2021/09716-5) and a Young Researcher Award (RAC, #2018/03910-1). CENAPAD-SP, CESUP and SDumont are also acknowledged for the computational resources used in theory calculations.

## Conflicts of interest

There are no conflicts to declare.

## References

- (a) C. Yu, A. Kütt, G.-V. Rösenthaller, T. Lebl, D. B. Cordes, A. M. Z. Slawin, M. Bühl and D. O'Hagan, *Angew. Chem., Int. Ed.*, 2020, **59**, 19905–19909; (b) D. O'Hagan, *Chem. – Eur. J.*, 2020, **26**, 7981–7997; (c) T. Bykova, N. Al-Maharik, A. M. Z. Slawin, M. Bühl, T. Lebl and D. O'Hagan, *Chem. – Eur. J.*, 2018, **24**, 13290–13296; (d) T. Bykova, N. Al-Maharik, A. M. Z. Slawin and D. O'Hagan, *Beilstein J. Org. Chem.*, 2017, **13**, 728–733; (e) M. Salah Ayoup, D. B. Cordes, A. M. Z. Slawin and D. O'Hagan, *Beilstein J. Org. Chem.*, 2015, **11**, 2671–2676.
- N. S. Keddie, A. M. Z. Slawin, T. Lebl, D. Philp and D. O'Hagan, *Nat. Chem.*, 2015, **7**, 483–488.
- (a) R. A. Cormanich, N. Keddie, R. Rittner, D. O'Hagan and M. Bühl, *Phys. Chem. Chem. Phys.*, 2015, **44**, 29475–29478; (b) B. E. Ziegler, M. Lecours, R. A. Marta, J. Featherstone, E. Fillion, W. S. Hopkins, V. Steinmetz, N. S. Keddie, D. O'Hagan and T. B. McMahon, *J. Am. Chem. Soc.*, 2016, **138**, 7460–7463; (c) M. J. Lecours, R. A. Marta, V. Steinmetz, N. Keddie, E. Fillion, D. O'Hagan, T. B. McMahon and W. S. Hopkins, *J. Phys. Chem. Lett.*, 2017, **8**, 109–113.
- (a) O. Shyshov, S. V. Haridas, L. Pesce, H. Y. Qi, A. Gardin, D. Bochicchio, U. Kaiser, G. M. Pavan and M. von Delius, *Nat. Commun.*, 2021, **12**, 3134; (b) A. Theodoridis, G. Papamokos, M. P. Wiesenfeldt, M. Wollenburg, K. Mullen, F. Glorius and G. Floudas, *J. Phys. Chem. B*, 2021, **125**, 3700–3709; (c) R. Mondal, M. Agbaria and Z. Nairoukh, *Chem. – Eur. J.*, 2021, **27**, 7193–7213.
- N. Santschi and R. Gilmour, *Nat. Chem.*, 2015, **7**, 467–468.
- (a) J. L. Clark, A. Taylor, A. Geddis, R. M. Neyyappadath, B. A. Piscelli, C. Yu, D. B. Cordes, A. M. Z. Slawin, R. A. Cormanich, S. Guldin and D. O'Hagan, *Chem. Sci.*, 2021, **12**, 9712–9719; (b) J. L. Clark, R. M. Neyyappadath, C. Yu, A. M. Z. Slawin, D. B. Cordes and D. O'Hagan, *Chem. – Eur. J.*, 2021, **27**, 16000–16005.
- H. Tsuji, G. Cantagrel, Y. Ueda, T. Chen, L. J. Wan and E. Nakamura, *Chem. – Asian J.*, 2013, **8**, 2377–2382.
- (a) T. Charvillat, P. Bernardelli, M. Daumas, X. Pannecoucke, V. Ferey and T. Besset, *Chem. Soc. Rev.*, 2021, **50**, 8178–8192; (b) Z. Nairoukh, M. Wollenburg, C. Schleppehorst, K. Bergander and F. Glorius, *Nat. Chem.*, 2019, **11**, 264–270; (c) M. P. Wiesenfeldt, Z. Nairoukh, W. Li and F. Glorius, *Science*, 2017, **357**, 908–912.
- (a) X. Zhang, L. Ling, M. Luo and X. Zeng, *Angew. Chem., Int. Ed.*, 2019, **58**, 16785–16789; (b) Y. Wei, B. Rao, X. Cong and X. Zeng, *J. Am. Chem. Soc.*, 2015, **137**, 9250–9253.
- (a) R. F. W. Bader, *Atoms in Molecules: A Quantum Theory*, Clarendon, Oxford, 1990; (b) J. Contreras-García, E. R. Johnson, S. Keinan, R. Chaudret, J. Piquemal, D. N. Beratan and W. Yang, *J. Chem. Theory Comput.*, 2011, **7**(3), 625–632; (c) A. Altun, F. Neese and G. Bistoni, *J. Chem. Theory Comput.*, 2019, **15**(11), 5894–5907.
- S. Yamada, M. Morita, Y. Wang, Q. Zhang, D. O'Hagan, T. Agou, H. Fukumoto, T. Kubota, M. Hara and T. Konno, *Crystals*, 2021, **11**, 450.

